
Be Persistent: Towards a Unified Solution for Mitigating Shortcuts in Deep Learning

Hadi M. Dolatabadi¹ Sarah M. Erfani¹ Christopher Leckie¹

Abstract

Deep neural networks (DNNs) are vulnerable to shortcut learning: rather than learning the intended task, they tend to draw inconclusive relationships between their inputs and outputs. Shortcut learning is ubiquitous among many failure cases of neural networks, and traces of this phenomenon can be seen in their generalizability issues, domain shift, adversarial vulnerability, and even bias towards majority groups. In this paper, we argue that this commonality in the cause of various DNN issues creates a significant opportunity that should be leveraged to find a unified solution for shortcut learning. To this end, we outline the recent advances in topological data analysis (TDA), and persistent homology (PH) in particular, to sketch a unified roadmap for detecting shortcuts in deep learning. We demonstrate our arguments by investigating the topological features of computational graphs in DNNs using two cases of unlearnable examples and bias in decision-making as our test studies. Our analysis of these two failure cases of DNNs reveals that finding a unified solution for shortcut learning in DNNs is not out of reach, and TDA can play a significant role in forming such a framework.

1. Introduction

Deep neural networks (DNNs) have reshaped the means of data processing and generation in the past decade. Many of the recent advances in different areas of machine learning, whether in natural language processing (Vaswani et al., 2017; Radford et al., 2018) or computer vision (He et al., 2016; Song & Ermon, 2019), can be attributed to the representational power of DNNs. For instance, it has been shown that neural networks can surpass human-level accuracy in

¹School of Computing and Information Systems, The University of Melbourne, Melbourne Connect, 700 Swanston Street, Carlton, 3053, Victoria, Australia. Correspondence to: Sarah M. Erfani <sarah.erfani@unimelb.edu.au>.

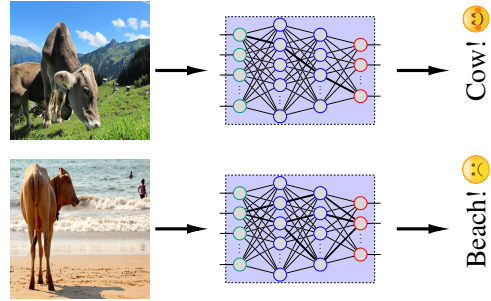


Figure 1. Neural networks exhibit spurious correlations, which is a special case of shortcut learning. For instance, DNN trained over data that depicted cows exclusively over grass has created a spurious correlation where cows are only detected in the presence of grass (Beery et al., 2018).

object detection (Russakovsky et al., 2015).

In contrast to humans, DNNs notoriously rely on spurious features and draw meaningless conclusions during decision-making (Beery et al., 2018; Singla & Feizi, 2022; Kirichenko et al., 2023). For instance, consider a DNN trained over a dataset that always depicts cows on the grass. Such a model considers grass as a spurious feature, and only detects cows where the background includes greenery (see Figure 1). This simple example indicates a serious flaw in DNNs’ decision-making, rendering it dangerous for sensitive applications to be at the mercy of neural networks (Wexler, 2017).

Spurious correlations are argued to be the result of a broader phenomenon known as *shortcut learning* (Geirhos et al., 2020). Shortcuts are unintended decision rules that are learned by neural networks (e.g., detecting grass instead of cows). These shortcuts are argued to be the result of following the “Principle of Least Effort” (Zipf, 1949) in which learning the unintended solution takes less effort compared to the actual task (Geirhos et al., 2020) (e.g., detecting greenery would be much easier than detecting cows in different colors and shapes). Various failure cases of neural networks, from domain shift (Wang & Deng, 2018) and adversarial examples (Szegedy et al., 2014) to even bias and fairness (Barocas et al., 2023), can be traced back to shortcut learning (Geirhos et al., 2020). This surprising alignment in the cause of these failure cases is a great opportunity that

should be leveraged towards finding a unified solution.

In this paper, we argue that topological data analysis (TDA) (Carlsson, 2009) can play an invaluable role in detecting and mitigating shortcuts in deep learning. In particular, we demonstrate that shortcut learning leaves tractable paths in the computational graph of a neural network. To unveil shortcuts in such a high-dimensional space containing thousands of neurons, we leverage the representational power of persistent homology (PH) (Edelsbrunner & Harer, 2008) in revealing connected components between neurons. We empirically show that neural networks that learn such shortcuts leave a signature in the topology of their computational graph. Our experiments reveal that these features are statistically different from those of benign neural networks.

To demonstrate our point, we choose two failure cases of DNNs in down-stream tasks: unlearnable examples (Huang et al., 2021; Yu et al., 2022) and bias (Buolamwini & Gebru, 2018; Du et al., 2021). Unlearnable examples are imperceptible perturbations added to the training data to prevent a DNN from learning meaningful patterns from the data (Huang et al., 2021; Dolatabadi et al., 2024). On the other hand, bias in neural networks can happen when a DNN misuses certain sensitive attributes from the data (such as skin color) to make its final decision (Buolamwini & Gebru, 2018). As seen, the origins of these two issues are quite different. However, we show that TDA can provide a unified means to shed light on both misbehaviors in DNNs. Our promising findings call for more research into the topological analysis of neural networks for treating shortcuts, with the hope that such a solution could mitigate various failures of DNNs once and for all.

Our contributions can be summarized as follows:

- We target shortcut learning as the main culprit among many failure cases of neural networks and argue that the research community should pay more attention to persistent homology to mitigate this issue. To the best of our knowledge, this is the first paper that proposes a unified roadmap for mitigating shortcut learning.
- We use two emerging issues in neural networks, namely unlearnable examples and bias in decision-making, as our case-studies to demonstrate the applicability of the same persistent homology framework to completely different issues in neural networks. Training more than a dozen models in each case, our experimental results demonstrate that persistent homology can easily reveal the differences between benign and affected models.
- Finally, we pinpoint some of the most important future research directions in this area that could lead to a unified solution for shortcut learning using persistent homology.

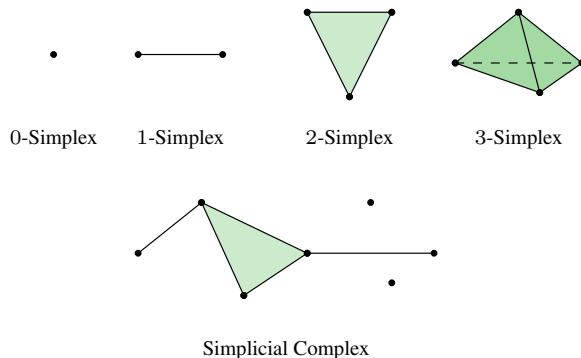


Figure 2. A k -Simplex can be regarded as the convex hull of $k + 1$ points. A simplicial complex is a union of such simplices.

2. Background

This section reviews the background related to persistent homology. Rather than an in-depth mathematical discussion, we focus on covering the intuition and a general understanding of persistent homology. We refer the interested reader to Edelsbrunner & Harer (2010) for a formal introduction to the topics discussed here.

2.1. Simplicial Homology

The field of computational topology (Edelsbrunner & Harer, 2010) is concerned with designing the mathematical tools required for finding topological features of low- and high-dimensional manifolds. To this end, the notion of *homology groups* in a *simplicial complex* is used. Informally speaking, a simplicial complex is a discretized graph representation of the data that contains information about nodes, edges, triangles, and their higher order equivalents (see Figure 2). A homology group of rank d , denoted by \mathcal{H}_d , is a d -dimensional topological descriptor for simplicial complexes. In this paper, we mainly work with 0- and 1-dimensional homology groups, which encode the number of connected components and cycles/loops in a simplicial complex.

2.2. Persistent Homology

Persistent homology (PH) (Barannikov, 1994; Edelsbrunner & Harer, 2008) extends the notion of simplicial homology to data observations. Rather than treating the data as samples from their true underlying manifold, PH aims to identify the most *persistent* topological structures within the data points, assuming noisy observations. To this end, the evolution of topological features at multiple granularities using a *filtration* is observed. A filtration creates a sequence of simplicial complexes at growing granularities, which enables us to track the evolution of topological features between consecutive levels of granularity. Each topological structure is created at a particular granularity and destroyed at another one. We refer to these as the birth and death times of our

topological features, respectively. We can then collect all these times as points in a 2-dimensional plane, creating a so-called *persistent diagram* (PD). Naturally, we would be interested in structures that have a long life-time/persistence (which is the subtraction of the death and birth time). This is because such structures are unlikely to have been generated by the noisy observations, and as such, are representing the true data manifold.

2.3. Vietoris-Rips Filtration

Vietoris-Rips (VR) (Vietoris, 1927) complex is a common method used for building a filtration of data points $\{\mathbf{a}_1, \mathbf{a}_2, \dots, \mathbf{a}_m\}$. To construct such a filtration, we start by defining a metric space over which we compare our data points using some notion of distance $d(\cdot, \cdot)$. At each scale ϵ , we connect all the data points that are within the ϵ distance of each other, i.e., data points that satisfy $d(\mathbf{a}_i, \mathbf{a}_j) \leq \epsilon$. We then sweep over all the possible ϵ 's from $-\infty$ to $+\infty$ and record the birth and death of topological features of interest in a PD. As mentioned earlier, in this paper we are mostly interested in capturing the 0D and 1D topological features. Thus, we would have a separate PD for each dimension. An illustrated example of finding the VR filtration for a set of point clouds is given in Figure 3.

3. Framework

This section presents our framework for the topological analysis of shortcut learning in neural networks. First, we formally introduce our problem setting and notation. Then, we go over the details of the topological analysis of neural networks for shortcut learning.

3.1. Problem Setting

Consider a labelled dataset $\mathcal{D} = \{(\mathbf{x}_i, y_i)\}_{i=1}^n$ where $\mathbf{x}_i \in \mathbb{R}^d$ and y_i denote a data sample and its associated label. Without loss of generality, in this paper, we consider a multi-class classification problem where y_i belongs to exactly one class from the set $\{1, 2, \dots, k\}$. Also, let $f_\theta : \mathbb{R}^d \rightarrow \mathbb{R}^k$ denote a neural network classifier with parameters θ that maps the inputs \mathbf{x} to a real-valued vector $\mathbf{z} \in \mathbb{R}^k$, commonly known as the *logit* vector. The final prediction of the classifier is obtained via solving $\hat{y} = \arg \max_c \mathbf{z}[c]$. To train the classifier f_θ , we usually optimize a relevant objective over the dataset:

$$\theta^* = \arg \min_{\theta} \sum_{i=1}^n \mathcal{L}(f_\theta(\mathbf{x}_i), y_i), \quad (1)$$

where $\mathcal{L}(\cdot, \cdot)$, called the loss function, is a measure of discrepancy between the prediction of the classifier and the ground-truth label. In this paper, we assume that our loss function is a cross-entropy function.

To pave the way for our discussion of topological analysis of DNNs, we need to define a few extra notations. Let m be the total number of neurons in a DNN. During inference, each input \mathbf{x}_i is sent through the neural network and processed by its neurons. Let $a_j^{(i)}$ denote the value of the j th neuron for the i th data sample \mathbf{x}_i . We gather the values of the j th neuron for N data samples in a so-called activation vector, written as:

$$\mathbf{a}_j = [a_j^{(1)}, a_j^{(2)}, \dots, a_j^{(N)}]^\top. \quad (2)$$

Using this notation, if we get the activation values of all the m neurons of the DNN for N data samples, we end up having a collection of m activation vectors $\mathcal{A} = \{\mathbf{a}_1, \mathbf{a}_2, \dots, \mathbf{a}_m\}$. Next, we will see how we can create a topological map of a neural network computation graph using the set \mathcal{A} .

3.2. Topological Analysis of Shortcut Learning

As mentioned before, shortcut learning is commonplace in neural networks. Intuitively, this phenomenon happens when a DNN learns an unusually direct path from its input to its output. We aim to reveal this unusual behavior by analyzing the traversal of input information through the computational graph of the neural network. We resort to PH for identifying this abnormal behavior in DNNs. To this end, we construct a VR filtration of the neural network computation graph following a method introduced in Zheng et al. (2021).

Recall from Section 2.3 that the first step during the construction of a VR filtration is to determine a meaningful distance measure between the data points. In our analysis, we are dealing with neurons as nodes in a computational graph. A shortcut happens when there are *multiple* neurons throughout the graph that are activated together. For this reason, we can use a standard correlation measure between the activation vectors of two different neurons as our distance metric in building a VR complex.

In other words, let us assume that \mathbf{a}_i and \mathbf{a}_j are two different activation vectors ($i \neq j$) constructed according to Equation (2). In addition, let $-1 \leq \rho(\mathbf{a}_i, \mathbf{a}_j) \leq 1$ be a normalized correlation metric between these two vectors. Then, we define the distance between these two activation vectors as:

$$d(\mathbf{a}_i, \mathbf{a}_j) = 1 - \rho(\mathbf{a}_i, \mathbf{a}_j). \quad (3)$$

This means that if the activation vectors \mathbf{a}_i and \mathbf{a}_j are highly correlated, their distance is smaller and vice versa.

Using this distance metric, we next build a VR filtration for the set of all neurons \mathcal{A} . To this end, we assume that each neuron is denoted by a node in a graph. Then, we sweep over ϵ from $-\infty$ to $+\infty$ and connect all the neurons whose activation vectors fall within an ϵ distance of each other.

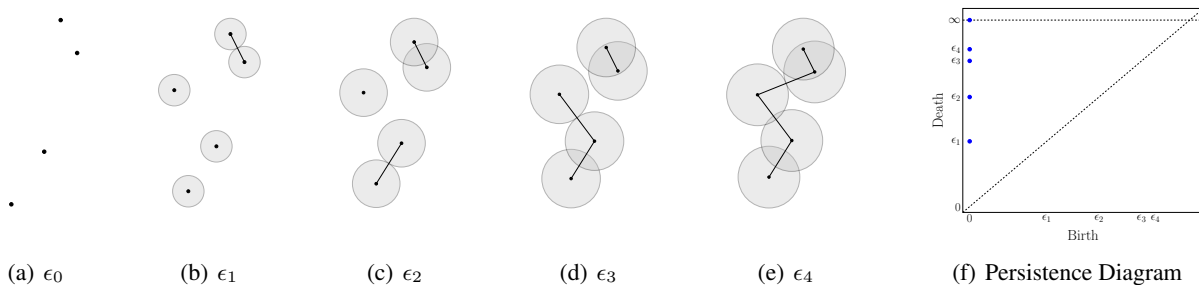


Figure 3. An example of computing the VR complex for a set of points in the Euclidean space. As the threshold increases, the 0-simplices gradually vanish. In the end, we would have only one connected component that lives forever.

This process would result in a filtration $\emptyset \subseteq \mathcal{G}_{\epsilon_1} \subseteq \mathcal{G}_{\epsilon_2} \subseteq \dots \subseteq \mathcal{G}_{\epsilon_\infty}$. Here, \mathcal{G}_{ϵ_i} is a graph representation of neurons, where the edges are connected to each other if they have a distance less than ϵ_i . We then use existing TDA tools to extract the 0D and 1D persistence diagrams of this filtration.

We are particularly interested in 1D topological structures, or cycles, in the computational graphs. This is because such structures capture a subset of neurons that are highly correlated with each other, meaning that they are often activated together. Remember that our activation vectors have been computed for N different inputs, and if N is large enough, such activation vectors should give us a fairly comprehensive overview of input traversal through neurons in a DNN. As such, finding a subset of neurons that are activated together (which could create a cycle in the topological features of computational graphs) can signal a shortcut path.

4. Case Studies

Now that we have established a framework for extracting the topological features of DNNs, in this section we show how the same framework is applicable to two different issues that both arise as a result of shortcut learning. We also present an extra case study on backdoor attacks in the Appendix.

4.1. Case Study I: Unlearnable Examples

4.1.1. OVERVIEW

Unlearnable examples (Huang et al., 2021), also known as availability attacks, are a family of data poisoning attacks (Biggio & Roli, 2018) aiming to protect personal data from being exploited. With the unauthorized access of third-party crawlers over the web, users might lose control over how their personal data is used for training deep neural networks such as automated facial recognition (Hill & Krolik, 2019; Hill, 2020). The goal of unlearnable examples is to passively prevent this misuse by adding an imperceptible perturbation to the user’s data before sharing it. This perturbation should be powerful enough not to let any DNN learn meaningful patterns from its underlying data, but impercep-

tible enough so it does not interfere with the utility of the data to be shared with its audience (Huang et al., 2021).

There are various ways to construct such data-protecting perturbations (Feng et al., 2019; Huang et al., 2021; Yuan & Wu, 2021; Fowl et al., 2021; Fu et al., 2022; Yu et al., 2022; Tian et al., 2022; Sandoval-Segura et al., 2022). In general, the goal of all these different approaches is to find a set of perturbations δ_i for each training data point x_i such that after optimizing the neural network weights over the perturbed data, the trained network yields a high error rate over the test set.¹ We can write this objective using our notations as:

$$\begin{aligned} \arg \max_{\{\delta_i \mid i \in \text{train}\}} \sum_{j \in \text{test}} \mathcal{L}(f_{\theta^*}(x_j), y_j) \\ \text{s.t. } \theta^* = \arg \min_{\theta} \sum_{i \in \text{train}} \mathcal{L}(f_{\theta}(x_i + \delta_i), y_i). \end{aligned} \quad (4)$$

Different methods opt to achieve this goal from different perspectives. One approach that is closely related to our analysis is presented in Yu et al. (2022). It is argued that the majority of existing unlearnable examples create shortcut paths within the neural network during training (Yu et al., 2022; Sandoval-Segura et al., 2023). As such, the perturbation generation process can be oversimplified, and even a set of linearly separable noisy data can act as unlearnable perturbations (Yu et al., 2022). Therefore, since unlearnable examples are related to shortcut learning in neural networks, they can be an interesting case study for our analysis.

4.1.2. EXPERIMENTAL EVALUATION

Settings: To empirically validate our speculations for the existence of a topological signature within DNNs trained over unlearnable datasets, we choose six state-of-the-art methods used for generating unlearnable perturbations. These approaches include Targeted Adversarial Poisoning (TAP) (Fowl et al., 2021), Error-minimizing Noise (EMN) (Huang et al., 2021), Robust

¹Note that the data protector might opt to protect only a subset of all the training data. In this case, we can simply set $\delta_i = \mathbf{0}$ for data samples that are not going to be protected.

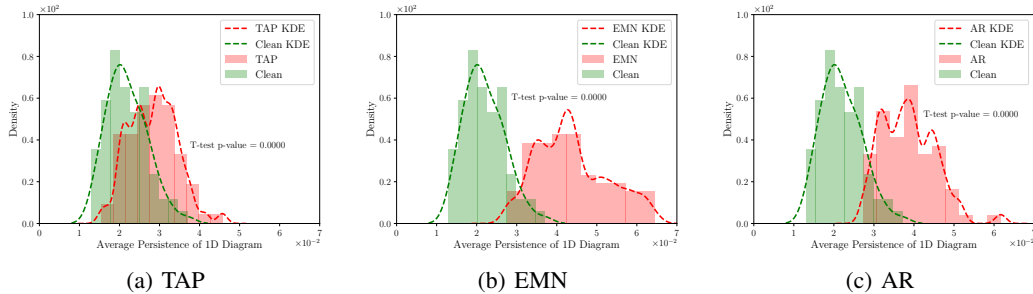


Figure 4. The distribution of average persistence of 1D homology groups for ResNet-18 models trained with different versions of unlearnable CIFAR-10 datasets. Each histogram summarizes the result of 70 independent training runs for each dataset. The p-value of the T-test has also been shown in each figure.

EMN (REM) (Fu et al., 2022), Neural Tangent Generalization Attacks (NTGA) (Yuan & Wu, 2021), Shortcut (SHR) (Geirhos et al., 2020), and Autoregressive attacks (AR) (Sandoval-Segura et al., 2022). Using these methods, we create unlearnable CIFAR-10 (Krizhevsky & Hinton, 2009) datasets and train 70 ResNet-18 (He et al., 2016) models over each dataset independently. Furthermore, we also train 70 ResNet-18 models over the clean version of the CIFAR-10 dataset. We use the settings used in Huang et al. (2021) for training our models.

Evaluation: After training each model until convergence, we use our framework outlined in Section 3 to extract topological features of the DNN computational graph. We use the `ripser` package (Tralie et al., 2018) to obtain the 1D persistence diagram (PD) of the computational graph using a VR filtration. Then, we operate over this PD for a statistical analysis of the topological features. To this end, we use the average life-span/persistence of the PD ($AVG PD_1$) as well as the Wasserstein distance (WSD) between a pair of PDs as our evaluation metrics (The GUDHI Project, 2015).

Findings: We can summarize our key findings as below:

- As shown in Figure 4, models trained on unlearnable datasets exhibit a different average persistence compared to clean models. The difference is statistically significant for all the tested unlearnable models, where the reported p-value is almost zero. This result demonstrates a clear distinguishing factor between benign and unlearnable models in their topological features, showing that **unlearnable datasets create alternative trajectories within the DNN for processing the inputs**. We report our results for the other unlearnable datasets in Figure 10 in the Appendix.
- Glancing at the highly persistent cycles within each model as shown in Figure 5, we can see that **unlearnable models block the flow of information from the clean test inputs**. Therefore, the models trained over unlearnable datasets should indeed exhibit a lower accu-

racy compared to the clean model. This observation can be verified by looking at the feature maps of the ResNet-18 models for a sample input. As shown in Figure 6, for unlearnable models we do not see any trace of the input during the intermediate layers, while this information is easily transferred to deeper layers of the clean DNN. For our results on other unlearnable examples, please see Figure 11 in the Appendix.

- Sandoval-Segura et al. (2023) argued that even unlearnable models capture useful features that can be utilized for a better classification. To this end, they used a simple linear classifier to train over the frozen feature extractor of such models with a small validation set. Kirichenko et al. (2023) earlier showed that this approach is useful in combating spurious correlations. Using the same approach, we train a linear classifier head to obtain a linear probe accuracy (LP ACC) for all our models. We also compute the Wasserstein distance between the PD of each model and a randomly sampled clean model. As can be seen in Figure 7, **there is a correspondence between the power of the unlearnable dataset and its ability to create alternative trajectories within the DNN**. In particular, a higher Wasserstein distance indicates that the trajectories of the trained model differ more from a baseline clean model. Therefore, models with a higher Wasserstein distance tend to have a lower LP accuracy, which shows that the underlying unlearnable dataset is more resilient. For an extended version of our results, please see the Appendix.

4.2. Case Study II: Bias and Fairness

4.2.1. OVERVIEW

Another interesting case of shortcut learning happens during the training of biased neural networks (Geirhos et al., 2020). It is widely known that bias usually takes place when a model focuses on one or a group of sensitive attributes to make its final prediction while ignoring the rest of input features (Barocas et al., 2023). Take the loan approval

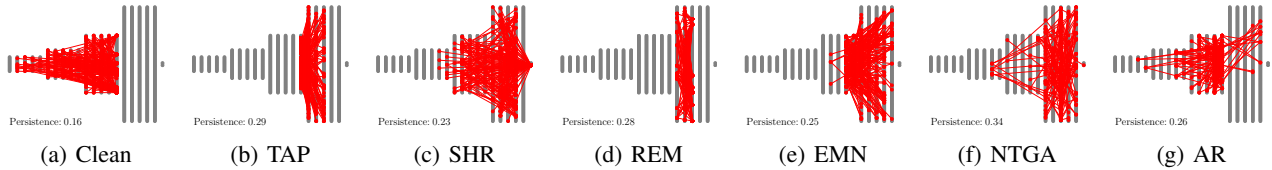


Figure 5. Top persistent cycle for one instance of ResNet-18 models trained with different versions of unlearnable CIFAR-10 datasets. Each node denotes a single neuron within the model. Note that due to the high number of neurons, we show a downsampled version of the original model.

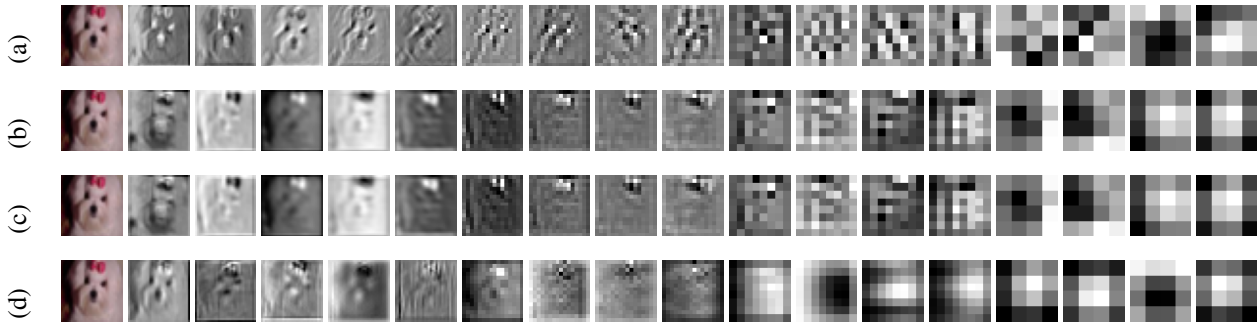


Figure 6. Feature space representation of one instance of ResNet-18 models trained with different versions of unlearnable CIFAR-10 datasets. The features are shown from the input space (leftmost) to the last layer of the classifier (rightmost). The models are trained using (a) clean, (b) TAP (Fowl et al., 2021), (c) EMN (Huang et al., 2021), and (d) AR (Sandoval-Segura et al., 2022) data.

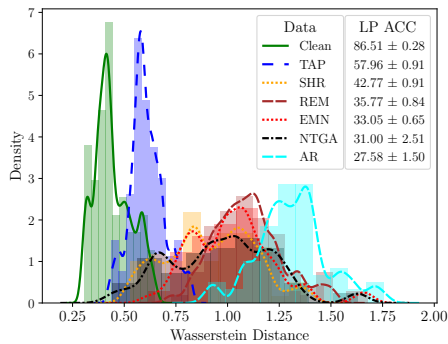


Figure 7. The Wasserstein distance between 1D persistence diagrams of clean versus unlearnable ResNet-18 models. For clean models, we compute the distance between two randomly selected models, while for unlearnable models we use a clean baseline.

application as an example. In this case, bias happens when the model puts extra focus on a certain sensitive attribute, like ZIP code, to decide whether a loan request should be approved or not (Du et al., 2021). Even though this notion is easy to comprehend, it is usually hard to track how the features are being processed within a machine learning model, especially when it comes to DNN models in the vision domain (Wang et al., 2019).

We can see traces of shortcut learning in the issue of bias and fairness in neural networks. Going back to our example of loan approvals, we can see that the ZIP code can act as a spurious feature: there exists a shortcut within the neural

network which is activated when certain sensitive ZIP codes appear as the input. For these ZIP codes, the model ignores the rest of the input features and outputs a negative decision. Even though this issue is quite different from the previous case study, we demonstrate that similar observations can be made through the lens of persistent homology.

4.2.2. EXPERIMENTAL EVALUATION

Settings: To conduct our empirical study, we use the state-of-the-art approach of Seo et al. (2022) to learn unbiased ResNet-18 models over the CelebA dataset (Liu et al., 2015). Using *gender* as our sensitive attribute, we train DNN models to predict various target attributes such as blonde hair, pale skin, etc. Naturally, these attributes have a skewed distribution depending on the subject’s gender. For instance, the CelebA dataset contains a higher number of blonde females in comparison to males, making it a great dataset to study fairness in DNNs. For each target attribute, we train 10 regular (biased) and fair (unbiased) models. The only exception is the “Blonde Hair”, for which we train 100 models.

Evaluation: To quantitatively evaluate bias in each case, we use common performance metrics such as unbiased accuracy, worst group accuracy, standard deviation of unbiased accuracy over groups, Equalized Odds (EO), and Average Odds (AO) (Barocas et al., 2023). Moreover, we use the framework outlined in Section 3 to calculate the topological

Table 1. Performance of ResNet-18 models trained over CelebA dataset with different target attributes. The sensitive attribute for all models is gender. In each case, we train a regular and an unbiased model using (Seo et al., 2022). The results are averaged over 10 models.

TARGET ATTRIBUTE	MODEL	PERFORMANCE METRICS					
		UNBIASED ACC (%)	WORST GROUP ACC (%)	UNBIASED ACC STD. (%)	EO DISPARITY (%)	AVERAGE ODDS (%)	TOP-5 1D PERS. ($\times 10^{-1}$)
BLONDE HAIR	BIASED	84.50 ± 1.35	54.81 ± 5.76	17.39 ± 2.56	37.13 ± 4.47	21.31 ± 2.23	1.38 ± 0.45
	UNBIASED	84.08 ± 2.26	78.20 ± 4.17	5.84 ± 2.31	12.89 ± 5.83	8.83 ± 4.39	0.88 ± 0.24
CHUBBY	BIASED	67.22 ± 1.73	22.24 ± 1.64	31.35 ± 1.81	32.13 ± 7.28	19.50 ± 4.59	1.06 ± 0.41
	UNBIASED	73.42 ± 2.24	61.53 ± 5.01	11.39 ± 2.85	19.53 ± 6.88	22.11 ± 6.28	0.70 ± 0.22
DOUBLE CHIN	BIASED	66.76 ± 2.96	21.02 ± 6.04	32.04 ± 3.55	32.10 ± 6.39	19.19 ± 4.06	1.05 ± 0.27
	UNBIASED	75.81 ± 1.49	65.58 ± 3.97	8.86 ± 2.76	14.65 ± 5.84	17.16 ± 5.66	0.74 ± 0.18
HEAVY MAKEUP	BIASED	74.58 ± 1.36	49.29 ± 4.05	22.05 ± 1.66	43.71 ± 5.29	43.59 ± 3.39	1.13 ± 0.27
	UNBIASED	74.69 ± 1.93	56.81 ± 2.35	15.62 ± 1.92	23.87 ± 6.02	29.47 ± 4.89	0.59 ± 0.19
OVAL FACE	BIASED	60.32 ± 1.20	20.03 ± 5.55	28.42 ± 4.38	29.51 ± 9.60	20.49 ± 8.19	0.77 ± 0.23
	UNBIASED	56.51 ± 3.97	48.84 ± 2.20	6.58 ± 2.37	11.24 ± 7.27	9.39 ± 6.29	0.66 ± 0.40
PALE SKIN	BIASED	80.49 ± 2.03	55.91 ± 5.39	17.83 ± 2.69	15.34 ± 3.84	8.65 ± 1.92	1.15 ± 0.17
	UNBIASED	86.96 ± 0.83	83.37 ± 1.61	2.99 ± 0.84	5.47 ± 2.73	4.94 ± 2.14	0.81 ± 0.19
POINTY NOSE	BIASED	63.96 ± 0.98	31.87 ± 4.24	22.12 ± 2.69	27.17 ± 3.82	22.79 ± 3.84	1.12 ± 0.41
	UNBIASED	62.27 ± 3.09	48.13 ± 6.07	12.69 ± 3.29	22.32 ± 8.46	24.15 ± 7.24	0.50 ± 0.19
STRAIGHT HAIR	BIASED	70.04 ± 1.46	52.58 ± 5.27	14.75 ± 4.82	7.18 ± 6.37	6.54 ± 3.02	0.88 ± 0.31
	UNBIASED	66.92 ± 1.84	57.43 ± 3.76	8.73 ± 2.96	12.05 ± 6.28	14.77 ± 6.31	0.65 ± 0.39
WEARING LIPSTICK	BIASED	77.79 ± 0.64	57.05 ± 1.79	18.73 ± 0.87	33.87 ± 2.74	37.20 ± 1.78	1.01 ± 0.21
	UNBIASED	73.59 ± 2.74	57.83 ± 7.36	14.82 ± 4.04	24.95 ± 11.55	28.47 ± 9.16	0.83 ± 0.19
YOUNG	BIASED	77.21 ± 0.58	55.16 ± 3.58	14.09 ± 1.91	12.59 ± 2.83	18.29 ± 2.74	0.95 ± 0.29
	UNBIASED	71.20 ± 1.75	62.67 ± 5.69	7.42 ± 4.12	14.42 ± 9.57	13.04 ± 9.02	0.89 ± 0.27

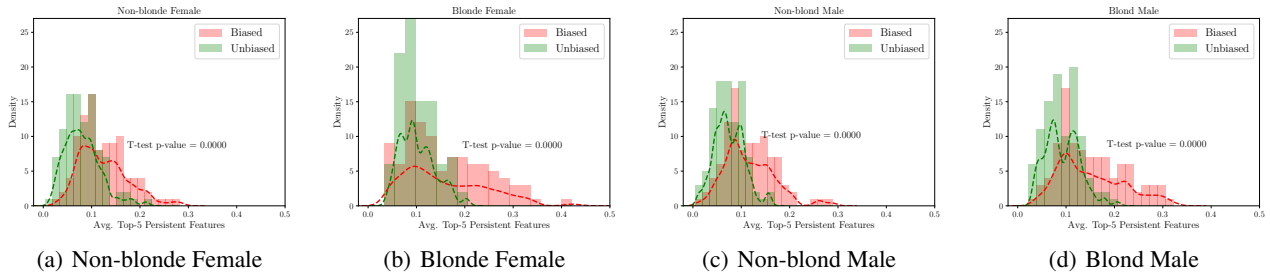


Figure 8. The distribution of average top-5 persistence of 1D homology groups for ResNet-18 models trained with biased and unbiased objectives. Each sub-figure represent a different protected group. The p-value of the T-test has also been shown in each figure.

features of each model. In particular, we compute the 1D persistence diagram of the model and obtain the mean of the top-5 persistent features.

Findings: We outline our key findings as below:

- As shown in Figure 8, **biased models exhibit a higher 1D persistence compared to unbiased models.** This has been likely caused by the discrepancies in the shortcut trajectories that biased models create within the DNN. Again, this difference is statistically significant to distinguish unbiased from biased models.
- We can see from Figure 9 that **models with higher top-**

5 persistence are more likely to be biased. This is also evident from the worst group accuracy of these models which are significantly lower than unbiased ones.

- In Table 1, we provide a quantitative comparison between biased and unbiased models for 10 target attributes from the CelebA dataset. As seen, all **unbiased models have a lower top-5 persistence compared to their biased counterparts.** Interestingly, a lower top-5 persistence signals a lower standard deviation for unbiased accuracy across sensitive groups. Therefore, **there exists a topological signature within DNN models that indicates whether they are biased or unbiased.**

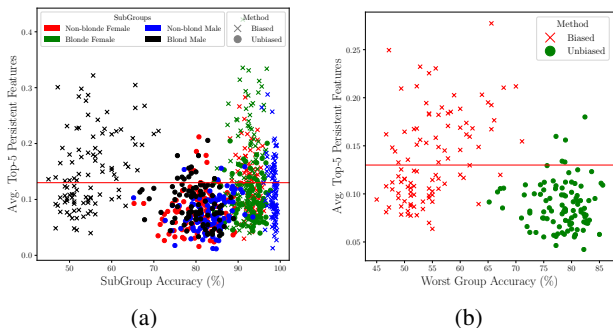


Figure 9. The scatter-plot of average top-5 persistence of 1D homology groups against (a) sub-group accuracy and (b) worst-group accuracy. The red line indicates a preset threshold that can separate the biased from unbiased models.

5. Conclusion and Future Directions

We demonstrated that the trajectories passed by inputs through neural networks contain invaluable insights about shortcuts within the model. To this end, we used two novel cases of shortcut learning in DNNs: unlearnable examples and fairness. We saw that persistent homology can play an important role in revealing these failure cases within a neural network. Interestingly, we showed that these differences are statistically significant.

While we used these two specific case studies, the application of persistent homology to such failure cases is not limited to these cases only. Previously, PH-based solutions have been independently discovered for other failures of neural networks related to shortcut learning, such as backdoor attacks (Zheng et al., 2021), adversarial examples (Gebhart & Schrater, 2017; Goibert et al., 2022), and out-of-distribution detection (Lacombe et al., 2021). In this paper, we aimed to argue that all such solutions can be combined to mitigate shortcut learning at a broader level. This is due to the fact that the cause of most issues with DNNs lie within shortcut learning, which could be traced by exploring the computational graphs trajectories. Below, we highlight interesting and challenging future directions:

- **Using Persistent Homology to Create Powerful Unlearnable Datasets:** As we see in Figure 7, the most resilient unlearnable examples are those that deviate the most from the usual trajectories of clean models. Proposing a novel unlearnable example generation objective that reflects such a phenomenon directly could lead to better unlearnable examples.
- **Proposing a New Fairness Measure based on Persistent Homology:** As we saw in Table 1, PH-based measures such as the top-5 persistent features have a tendency towards revealing bias in DNN models. However, these raw measures are not calibrated: even though their relative magnitude could be an indication of bias,

we cannot directly compare different models based on this measure. Introducing a new calibrated measure of fairness using persistent homology could be helpful in a better, more universal quantification of fairness in DNN models.

- **Incorporating Topological Measures in Decision-Making:** In a broader sense, quantification of uncertainty using topological measures could become the cornerstone of decision-making using DNNs. This is because apparently normal models should guide the inputs in certain trajectories within the network, and as such, proposing a new measure that covers this could help us detect issues within a neural network in a straightforward manner. Such solutions have also the potential of explainability, as they could reveal the paths involved with a given input during inference.
- **Introducing a Universal Regularizer for DNN Training:** Once we can quantify a universal measure for quantification of uncertainty, we could potentially use these measures to enforce certain behavior within the neural network computational graph. Unfortunately, existing tools for integrating topological measures during neural network training lag behind their counterparts in terms of their computational speed (Hofer et al., 2020), rendering it challenging to use for large-scale models.
- **Testing Solutions under Different Shortcut Learning Scenarios:** Lastly, we encourage researchers in this area to test their solutions not only for a specific type of shortcuts, but for a broad range of them. The creation of a standard benchmark along this line could help researchers to think about the broader issue of shortcut learning rather than focusing on a specific use case.

Broader Societal Impact

In this paper, we present our arguments as to why the machine learning community should pay more attention to topological data analysis for a unified treatment of shortcut learning. We believe that by doing so, we can address many shortcomings of current neural network models, including fairness, adversarial robustness, and backdoor attacks. While the intention of our work is to advance the field of deep learning, it may have potential societal impacts. For example, a malicious actor might decide to negate the impact of unlearnable examples on privacy, and train illegal facial recognition models on users’ data without their consent. That being said, we do not believe that such potential negative impacts need to be discussed in detail here, as the main goal of this work is to enhance the reliability of neural network models for good.

References

- Barannikov, S. The framed morse complex and its invariants. *Advances in Soviet Mathematics*, 21:93–116, 1994.
- Barocas, S., Hardt, M., and Narayanan, A. *Fairness and Machine Learning: Limitations and Opportunities*. MIT Press, Cambridge, Massachusetts, United States, 2023.
- Beery, S., Horn, G. V., and Perona, P. Recognition in terra incognita. In *European Conference on Computer Vision (ECCV)*, pp. 472–489, 2018.
- Biggio, B. and Roli, F. Wild patterns: Ten years after the rise of adversarial machine learning. *Pattern Recognition*, 84:317–331, 2018.
- Buolamwini, J. and Gebru, T. Gender shades: Intersectional accuracy disparities in commercial gender classification. In *Proceedings of the Conference on Fairness, Accountability and Transparency (FAccT)*, 2018.
- Carlsson, G. Topology and data. *Bulletin of the American Mathematical Society (AMS)*, 46(2):255–308, 2009.
- Chen, X., Liu, C., Li, B., Lu, K., and Song, D. Targeted backdoor attacks on deep learning systems using data poisoning. *CoRR*, abs/1712.05526, 2017.
- Dolatabadi, H. M., Erfani, S. M., and Leckie, C. The devil’s advocate: Shattering the illusion of unexploitable data using diffusion models. In *IEEE Conference on Secure and Trustworthy Machine Learning (SatML)*, 2024.
- Du, M., Yang, F., Zou, N., and Hu, X. Fairness in deep learning: A computational perspective. *IEEE Intelligent Systems*, 36(4):25–34, 2021.
- Edelsbrunner, H. and Harer, J. Persistent homology—a survey. *Contemporary mathematics*, 453(26):257–282, 2008.
- Edelsbrunner, H. and Harer, J. *Computational Topology - an Introduction*. American Mathematical Society, Providence, Rhode Island, United States, 2010.
- Feng, J., Cai, Q., and Zhou, Z. Learning to confuse: Generating training time adversarial data with auto-encoder. In *Advances in Neural Information Processing Systems 32: Annual Conference on Neural Information Processing Systems (NeurIPS)*, pp. 11971–11981, 2019.
- Fowl, L., Goldblum, M., Chiang, P., Geiping, J., Czaja, W., and Goldstein, T. Adversarial examples make strong poisons. In *Proceedings of the Advances in Neural Information Processing Systems 34: Annual Conference on Neural Information Processing Systems (NeurIPS)*, pp. 30339–30351, 2021.
- Fu, S., He, F., Liu, Y., Shen, L., and Tao, D. Robust unlearnable examples: Protecting data privacy against adversarial learning. In *Proceedings of the 10th International Conference on Learning Representations (ICLR)*, 2022.
- Gebhart, T. and Schrater, P. Adversary detection in neural networks via persistent homology. *CoRR*, abs/1711.10056, 2017.
- Geirhos, R., Jacobsen, J., Michaelis, C., Zemel, R. S., Brendel, W., Bethge, M., and Wichmann, F. A. Shortcut learning in deep neural networks. *Nature Machine Intelligence*, 2(11):665–673, 2020.
- Goibert, M., Ricatte, T., and Dohmatob, E. An adversarial robustness perspective on the topology of neural networks. In *Proceedings of the Machine Learning Safety Workshop, Conference on Neural Information Processing Systems (NeurIPS)*, 2022.
- Gu, T., Dolan-Gavitt, B., and Garg, S. BadNets: Identifying vulnerabilities in the machine learning model supply chain. *CoRR*, abs/1708.06733, 2017.
- He, K., Zhang, X., Ren, S., and Sun, J. Deep residual learning for image recognition. In *Proceedings of the IEEE Conference on Computer Vision and Pattern Recognition (CVPR)*, pp. 770–778, 2016.
- Hill, K. The secretive company that might end privacy as we know it. *The New York Times*, 2020.
- Hill, K. and Krolik, A. How photos of your kids are powering surveillance technology. *The New York Times*, 2019.
- Hofer, C. D., Graf, F., Niethammer, M., and Kwitt, R. Topologically densified distributions. In *Proceedings of the 37th International Conference on Machine Learning (ICML)*, pp. 4304–4313, 2020.
- Huang, G., Liu, Z., van der Maaten, L., and Weinberger, K. Q. Densely connected convolutional networks. In *Proceedings of the IEEE Conference on Computer Vision and Pattern Recognition (CVPR)*, pp. 2261–2269, 2017.
- Huang, H., Ma, X., Erfani, S. M., Bailey, J., and Wang, Y. Unlearnable examples: Making personal data unexploitable. In *Proceedings of the 9th International Conference on Learning Representations (ICLR)*, 2021.
- Kirichenko, P., Izmailov, P., and Wilson, A. G. Last layer re-training is sufficient for robustness to spurious correlations. In *The 11th International Conference on Learning Representations (ICLR)*, 2023.
- Krizhevsky, A. and Hinton, G. Learning multiple layers of features from tiny images. Master’s thesis, Department of Computer Science, University of Toronto, 2009.

- Lacombe, T., Ike, Y., Carrière, M., Chazal, F., Glisse, M., and Umeda, Y. Topological uncertainty: Monitoring trained neural networks through persistence of activation graphs. In *Proceedings of the 13th International Joint Conference on Artificial Intelligence (IJCAI)*, pp. 2666–2672, 2021.
- Li, Y., Li, Y., Wu, B., Li, L., He, R., and Lyu, S. Invisible backdoor attack with sample-specific triggers. In *Proceedings of the IEEE/CVF International Conference on Computer Vision (ICCV)*, pp. 16443–16452, 2021a.
- Li, Y., Zhai, T., Jiang, Y., Li, Z., and Xia, S. Backdoor attack in the physical world. *CoRR*, abs/2104.02361, 2021b.
- Li, Y., Ya, M., Bai, Y., Jiang, Y., and Xia, S.-T. BackdoorBox: A python toolbox for backdoor learning. In *Proceedings of the ICLR Workshop on Backdoor Attacks and Defenses in Machine Learning*, 2023.
- Liu, Y., Ma, X., Bailey, J., and Lu, F. Reflection backdoor: A natural backdoor attack on deep neural networks. In *Proceedings of the 16th European Conference on Computer Vision (ECCV)*, 2020.
- Liu, Z., Luo, P., Wang, X., and Tang, X. Deep learning face attributes in the wild. In *Proceedings of International Conference on Computer Vision (ICCV)*, 2015.
- Nguyen, T. A. and Tran, A. T. Input-aware dynamic backdoor attack. In *Advances in Neural Information Processing Systems 33: Annual Conference on Neural Information Processing Systems (NeurIPS)*, 2020.
- Nguyen, T. A. and Tran, A. T. WaNet - imperceptible warping-based backdoor attack. In *Proceedings of the 9th International Conference on Learning Representations (ICLR)*, 2021.
- Radford, A., Narasimhan, K., Salimans, T., Sutskever, I., et al. Improving language understanding by generative pre-training. 2018.
- Russakovsky, O., Deng, J., Su, H., Krause, J., Satheesh, S., Ma, S., Huang, Z., Karpathy, A., Khosla, A., Bernstein, M. S., Berg, A. C., and Li, F. ImageNet large scale visual recognition challenge. *International Journal of Computer Vision (IJCV)*, 115(3):211–252, 2015.
- Sandoval-Segura, P., Singla, V., Geiping, J., Goldblum, M., Goldstein, T., and Jacobs, D. W. Autoregressive perturbations for data poisoning. In *Advances in Neural Information Processing Systems 35: Annual Conference on Neural Information Processing Systems (NeurIPS)*, 2022.
- Sandoval-Segura, P., Singla, V., Geiping, J., Goldblum, M., and Goldstein, T. What can we learn from unlearnable datasets? In *Proceedings of the Advances in Neural Information Processing Systems 36: Annual Conference on Neural Information Processing Systems (NeurIPS)*, 2023.
- Seo, S., Lee, J., and Han, B. Unsupervised learning of debiased representations with pseudo-attributes. In *Proceedings of the IEEE/CVF Conference on Computer Vision and Pattern Recognition (CVPR)*, pp. 16721–16730, 2022.
- Singla, S. and Feizi, S. Salient ImageNet: How to discover spurious features in deep learning? In *The 10th International Conference on Learning Representations (ICLR)*, 2022.
- Song, Y. and Ermon, S. Generative modeling by estimating gradients of the data distribution. In *Advances in Neural Information Processing Systems 32: Annual Conference on Neural Information Processing Systems (NeurIPS)*, pp. 11895–11907, 2019.
- Szegedy, C., Zaremba, W., Sutskever, I., Bruna, J., Erhan, D., Goodfellow, I. J., and Fergus, R. Intriguing properties of neural networks. In *Proceedings of the 2nd International Conference on Learning Representations (ICLR)*, 2014.
- The GUDHI Project. *GUDHI User and Reference Manual*. GUDHI Editorial Board, 2015. URL <http://gudhi.gforge.inria.fr/doc/latest/>.
- Tian, Q., Kuang, K., Jiang, K., Liu, F., Wang, Z., and Wu, F. ConfounderGAN: Protecting image data privacy with causal confounder. In *Advances in Neural Information Processing Systems 35: Annual Conference on Neural Information Processing Systems (NeurIPS)*, 2022.
- Tralie, C., Saul, N., and Bar-On, R. Ripser.py: A lean persistent homology library for python. *The Journal of Open Source Software*, 3(29):925, Sep 2018.
- Turner, A., Tsipras, D., and Madry, A. Label-consistent backdoor attacks. *CoRR*, abs/1912.02771, 2019.
- Vaswani, A., Shazeer, N., Parmar, N., Uszkoreit, J., Jones, L., Gomez, A. N., Kaiser, L., and Polosukhin, I. Attention is all you need. In *Proceedings of the Advances in Neural Information Processing Systems 30: Annual Conference on Neural Information Processing Systems (NeurIPS)*, pp. 5998–6008, 2017.
- Vietoris, L. Über den höheren zusammenhang kompakter räume und eine klasse von zusammenhangstreuen abbildungen. *Mathematische Annalen*, 97(1):454–472, 1927.
- Wang, M. and Deng, W. Deep visual domain adaptation: A survey. *Neurocomputing*, 312:135–153, 2018.

- Wang, T., Zhao, J., Yatskar, M., Chang, K., and Ordonez, V. Balanced datasets are not enough: Estimating and mitigating gender bias in deep image representations. In *Proceedings of the IEEE/CVF International Conference on Computer Vision (ICCV)*, pp. 5309–5318, 2019.
- Wexler, R. When a computer program keeps you in jail: How computers are harming criminal justice. *New York Times*, 13, 2017.
- Yu, D., Zhang, H., Chen, W., Yin, J., and Liu, T. Availability attacks create shortcuts. In *Proceedings of the 28th ACM SIGKDD Conference on Knowledge Discovery and Data Mining*, pp. 2367–2376, 2022.
- Yuan, C. and Wu, S. Neural tangent generalization attacks. In *Proceedings of the 38th International Conference on Machine Learning (ICML)*, pp. 12230–12240, 2021.
- Zheng, S., Zhang, Y., Wagner, H., Goswami, M., and Chen, C. Topological detection of trojaned neural networks. In *Proceedings of the Advances in Neural Information Processing Systems 34: Annual Conference on Neural Information Processing Systems 2021 (NeurIPS)*, pp. 17258–17272, 2021.
- Zipf, G. K. *Human behavior and the principle of least effort*. Addison-Wesley Press, Boston, Massachusetts, United States, 1949.

A. Extended Experimental Results

In this section, we present an extended version of our experimental results on unlearnable examples in Section 4.1.

In Figure 4, we presented the distribution of average persistence of 1D persistence diagrams (PDs) for models trained over three unlearnable datasets. Figure 10 shows our full results for all of the six unlearnable datasets considered in this paper. As seen, in all unlearnable models, the population of the topological measure is statistically different from that of clean models. This signals that inputs in unlearnable models traverse a different trajectory compared to clean models. To demonstrate this point, we show the top-3 persistent cycles (the ones with the highest life-time) for each unlearnable model along with the clean model in Figure 12: The trajectories traversed by inputs in the clean model are quite different from those of unlearnable models. Interestingly, as depicted in Figure 11, these trajectories indicate how the features from input progresses through the model. In the clean model, we can clearly spot the features of the input image in the intermediate layers of the network, while this is not the case for all the unlearnable models. This point is also clearly visible from the top-3 trajectories shown in Figure 12.

In Section 4.1, we also investigated how topological data analysis can reveal the power of an unlearnable dataset. In particular, we showed that as the Wasserstein distance between the persistence diagram of the poisoned model and that of the clean model increases, the linear probe accuracy (LP ACC) of that model decreases. We report similar observations for DenseNet-121 (Huang et al., 2017) as another DNN architecture. We use exactly the same settings as the ResNet-18 for this architecture, and train 70 independent models for each unlearnable dataset plus the clean one. Then, we use the fine-tuning approach of Sandoval-Segura et al. (2023) to obtain a linear probe accuracy. Figure 13 and Table 2 show our results. As seen, we can make the same conclusions about the Wasserstein distance and its relationship with the power of unlearnable examples for the DenseNet-121 models.

B. Extra Case Study: Backdoor Attacks

Backdoor attacks (Gu et al., 2017) are a family of data poisoning attacks where the adversary implants a backdoor in the model through poisoning the training data. This is usually done via attaching certain triggers to some of the training data. The adversary’s goal is to ensure that the poisoned model behaves normally under benign inputs while outputting its intended outcome whenever the trigger is activated. There have been numerous backdoor attacks such as BadNets (Gu et al., 2017), Blended (Chen et al., 2017), PhysicalBA (Li et al., 2021b), Label-Consistence (LC) (Turner et al., 2019), Reflection Backdoor (Refool) (Liu et al., 2020), ISSBA (Li et al., 2021a), Input-aware Dynamic Backdoors (IAD) (Nguyen & Tran, 2020), and WaNet (Nguyen & Tran, 2021) that were proposed to create powerful and stealthy backdoors against neural networks.

It has been commonly believed that backdoor attacks also create a shortcut within the neural network, and that this shortcut is activated whenever the input contains the trigger. Zheng et al. (2021) used this informal belief and devised a topological feature extractor to detect poisoned from benign models. In this section, we extend our statistical analysis for unlearnable datasets to backdoor attacks. To this end, we use the `BackdoorBox` (Li et al., 2023) library² and train 70 ResNet-18 models on the CIFAR-10 dataset for each of the previously mentioned backdoor attacks as well the clean data. Then, we use the same topological framework of Zheng et al. (2021) to extract the topological features of the trained models.

Table 3 and Figure 14 summarize our experimental results on backdoor attacks. Similar to the previous two case studies, we see that almost all backdoor attacks leave topological signatures within the neural network trajectories and persistent homology can reveal them. Similar to the other two cases, if we can come up with a differentiable topological regularizer for neural networks, we might be able to mitigate backdoor attacks as well. As we can see, for all the three case studies, the same topological tool can be applied. This is because the root cause of all these issues traces back to shortcut learning, which is a malicious behavior in neural networks.

²<https://github.com/THUYimingLi/BackdoorBox>

Table 2. Performance of ResNet-18 and DenseNet-121 models trained over data availability attacks on CIFAR-10 dataset. The performance over the clean dataset is shown for reference. The results are averaged over 70 models. LP and AVG PD₁ stand for Linear Probe and Average Persistence of 1D diagram, respectively.

ARCH	DATASET	PERFORMANCE METRICS				
		TRAIN ACC (%)	TEST ACC (%)	LP ACC (%)	AVG PD ₁ ($\times 10^{-2}$)	WSD
RESNET-18	CLEAN	97.44 \pm 0.00	86.78 \pm 0.25	86.51 \pm 0.28	2.19 \pm 0.50	0.44 \pm 0.10
	TAP	100.0 \pm 0.00	17.71 \pm 1.81	57.96 \pm 0.90	2.84 \pm 0.60	0.61 \pm 0.08
	SHR	100.0 \pm 0.00	12.59 \pm 1.55	42.77 \pm 0.91	3.10 \pm 0.69	0.92 \pm 0.21
	REM	100.0 \pm 0.00	21.95 \pm 1.52	35.77 \pm 0.84	3.80 \pm 0.77	1.10 \pm 0.16
	EMN	100.0 \pm 0.00	20.83 \pm 0.40	33.05 \pm 0.65	4.39 \pm 0.90	1.02 \pm 0.20
	NTGA	100.0 \pm 0.00	12.69 \pm 2.42	31.00 \pm 2.51	3.32 \pm 0.62	0.97 \pm 0.25
	AR	100.0 \pm 0.00	13.21 \pm 1.37	27.58 \pm 1.50	3.86 \pm 0.67	1.31 \pm 0.17
DENSENET-121	CLEAN	97.44 \pm 0.00	95.05 \pm 0.15	94.93 \pm 0.15	2.70 \pm 0.30	1.98 \pm 0.30
	TAP	100.0 \pm 0.00	13.13 \pm 1.41	72.10 \pm 0.49	2.38 \pm 0.26	2.16 \pm 0.28
	EMN	100.0 \pm 0.00	24.15 \pm 0.92	54.28 \pm 1.55	2.41 \pm 0.24	2.61 \pm 0.33
	NTGA	100.0 \pm 0.00	13.74 \pm 4.19	51.88 \pm 3.37	2.51 \pm 0.29	3.11 \pm 0.48
	SHR	100.0 \pm 0.00	15.33 \pm 1.33	50.29 \pm 1.07	2.51 \pm 0.29	3.11 \pm 0.39
	REM	100.0 \pm 0.00	20.34 \pm 1.57	43.29 \pm 0.78	2.89 \pm 0.18	4.69 \pm 0.46
	AR	100.0 \pm 0.00	13.23 \pm 1.49	32.55 \pm 1.98	2.96 \pm 0.30	4.75 \pm 0.58

Table 3. Performance of ResNet-18 models trained over various backdoor attacks on CIFAR-10 dataset. The performance over the benign dataset is shown for reference. The results are averaged over 70 models.

ARCH	ATTACK	PERFORMANCE METRICS		
		TEST ACC (%)	BACKDOOR ACC (%)	AVG TOP-5 PD ₁ ($\times 10^{-1}$)
RESNET-18	BENIGN	91.49 \pm 0.29	—	0.99 \pm 0.25
	WANET	90.42 \pm 0.25	98.62 \pm 0.73	1.08 \pm 0.36
	BLENDED	90.55 \pm 0.32	83.84 \pm 0.68	1.19 \pm 0.29
	PHYSICALBA	93.54 \pm 0.22	96.56 \pm 0.32	1.27 \pm 0.29
	REFOOL	90.98 \pm 0.29	96.68 \pm 0.44	1.38 \pm 0.38
	ISSBA	94.36 \pm 0.17	99.85 \pm 0.35	1.55 \pm 0.26
	IAD	93.88 \pm 0.16	96.63 \pm 1.37	1.64 \pm 0.34
	BADNETS	91.17 \pm 0.26	97.29 \pm 0.11	1.76 \pm 0.32
	LC	91.53 \pm 0.30	99.80 \pm 0.38	1.95 \pm 0.29

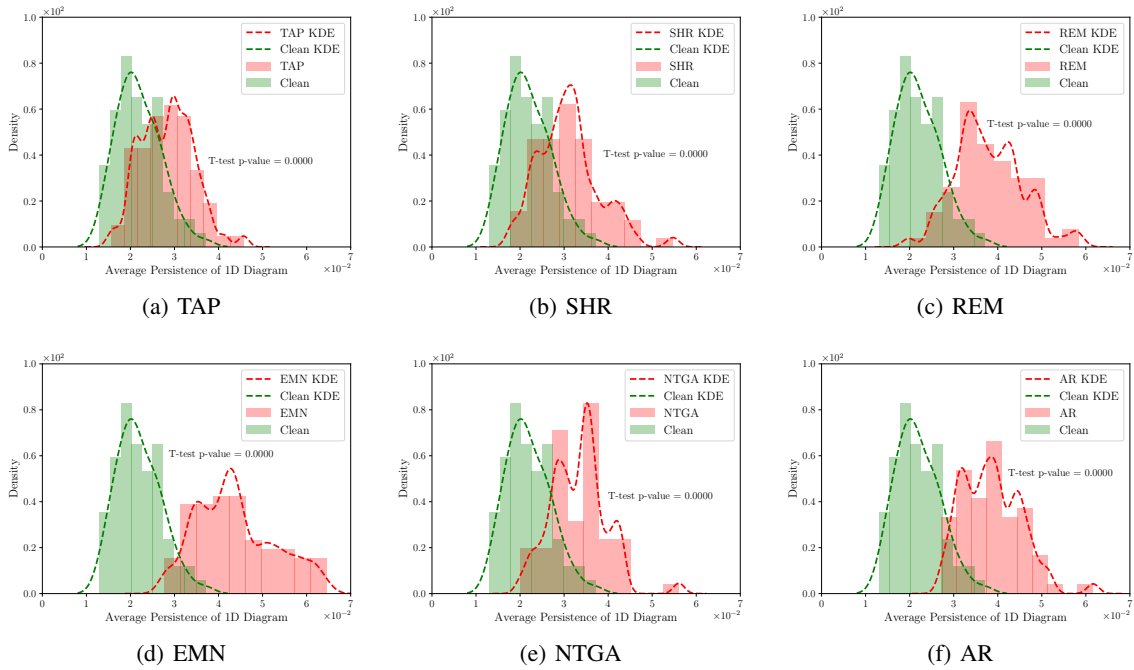


Figure 10. The distribution of average persistence of 1D homology groups for ResNet-18 models trained with different versions of unlearnable CIFAR-10 datasets. Each histogram summarizes the result of 70 independent training runs for each dataset. The p-value of the T-test has also been shown in each figure.

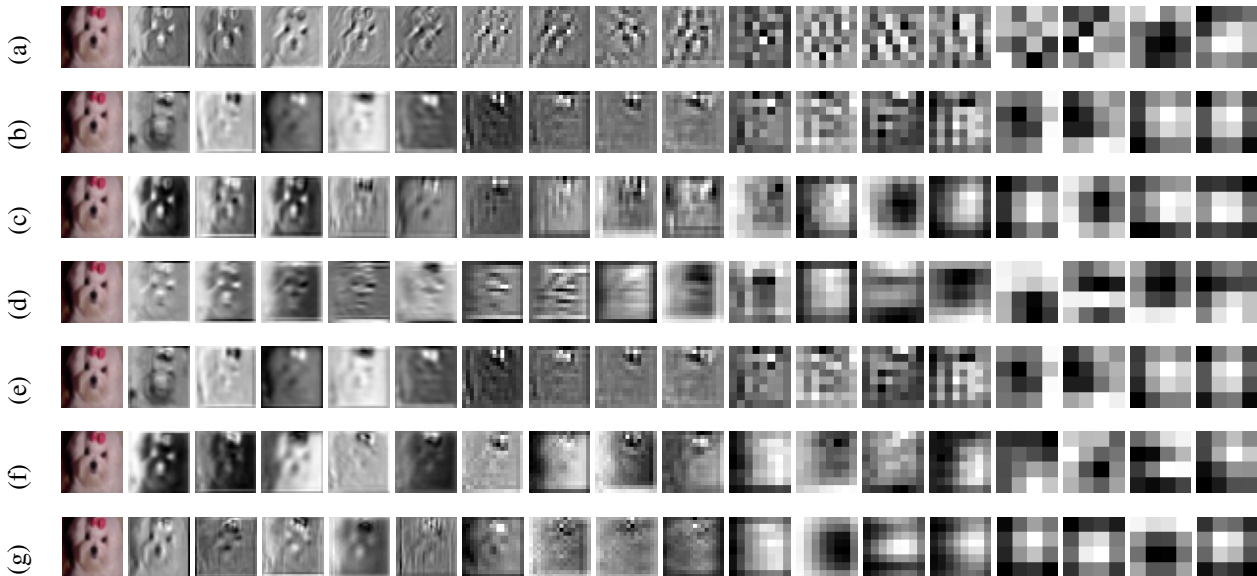


Figure 11. Feature space representation of one instance of ResNet-18 models trained with different versions of unlearnable CIFAR-10 datasets. The features are shown from the input space (leftmost) to the last layer of the classifier (rightmost). The models are trained using (a) clean, (b) TAP (Fowl et al., 2021), (c) SHR (Yu et al., 2022), (d) REM (Fu et al., 2022) (e) EMN (Huang et al., 2021), (f) NTGA (Yuan & Wu, 2021), and (g) AR (Sandoval-Segura et al., 2022) data.

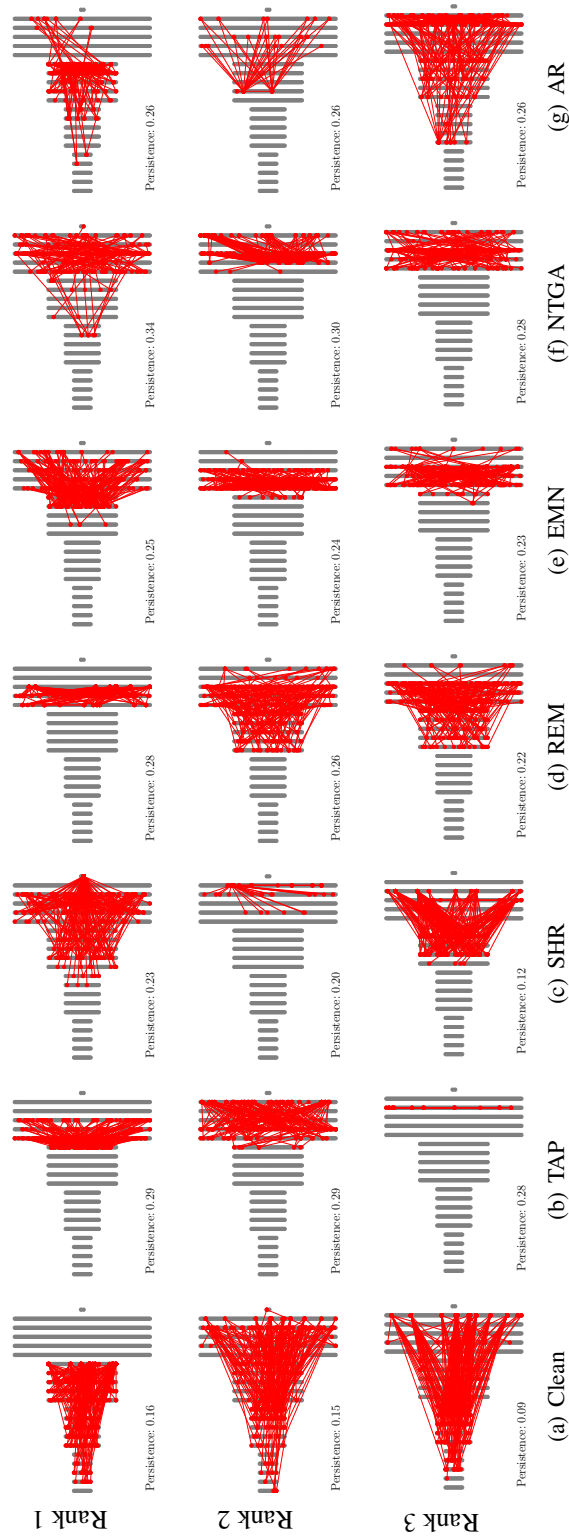


Figure 12. Top-3 persistent cycles for one instance of ResNet-18 models trained with different versions of unlearnable CIFAR-10 datasets. Each node denotes a single neuron within the model. Note that due to the high number of neurons, we show a downsampled version of the original model.

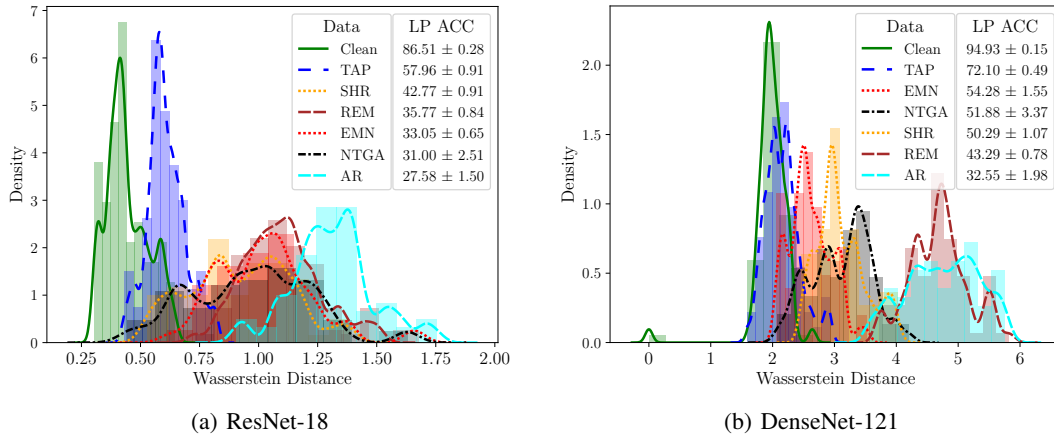


Figure 13. The Wasserstein distance between 1D persistence diagrams of clean versus unlearnable (a) ResNet-18 and (b) DenseNet-121 models. For clean models, we compute the distance between two randomly selected models, while for unlearnable models we use a clean baseline.

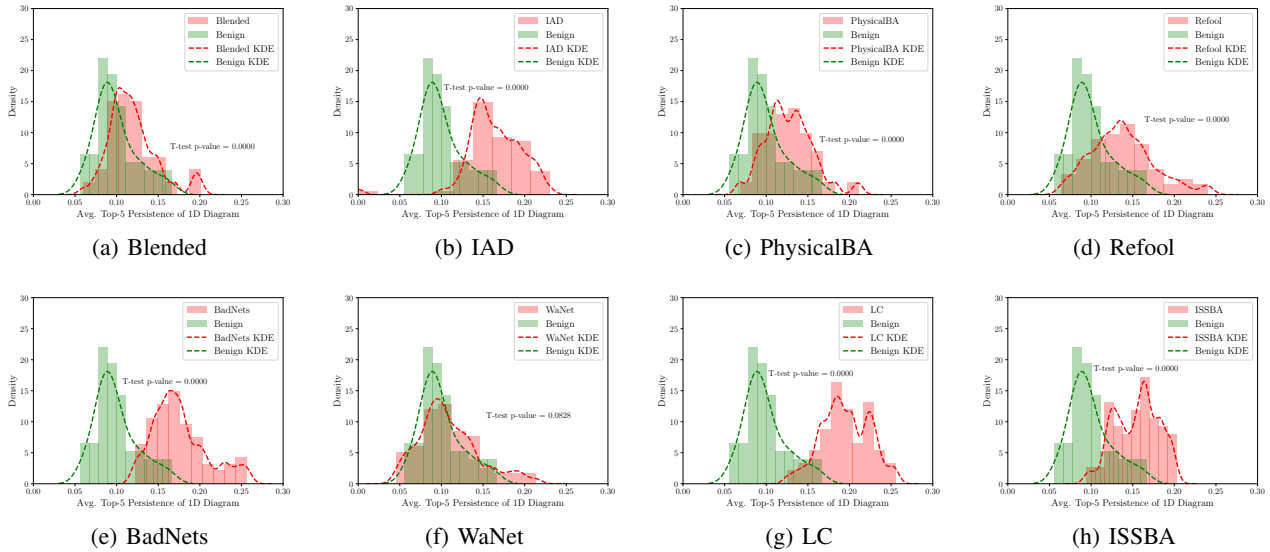


Figure 14. The distribution of average top-5 persistence of 1D homology groups for ResNet-18 models trained over various backdoored CIFAR-10 datasets. Each histogram summarizes the result of 70 independent training runs for each dataset. The p-value of the T-test has also been shown in each figure.